CHITOSAN NANOPARTICLE ENCAPSULATED WITH *Terminalia chebula* – *in vitro* ANTIDIABETIC ACTIVITY

RAHUL NATH, K. RAJAKUMARI*, R. THIRUCHELVI, S. IVO ROMAULD, P. VIVEK

Department of Bio-Engineering, School of Engineering, Vels Institute of Science, Technology and Advanced Studies, Pallavaram, 600 117 Chennai, Tamil Nadu, India
E-mail: *rajikumari91@gmail.com*

ABSTRACT

Terminalia chebula is an ayurveda herb which is used as the traditional medicinal plant and provide an adverse effect in treating the disease. It is widely used in the treatment of glucose- related diseases. The chitosan is a polymer that can be easily available in the form of biocompatible and non-toxic in nature. It can be used as a biodegradable polymer and drug delivery in the pharmaceutical industry. The detection of chitosan nanoparticle was carried out by characterisation methods like UV-Vis. Spectroscopy, FE-SEM, EDS, FT-IR, XRD and DLS. Alpha amylase assay and alpha glycosidase assay (glucose tolerance test) have been done for antidiabetic activity. The glucose metabolism and the viability of cells have been performed through 3-(4,5-dimethylthiazol-2-yl)-2,5-diphenyl-2H-tetrazolium bromide (MTT) assay. Here the 3T3 fibroblastic cell line has been used. The glucose metabolism also confirms that the drug morphology and binding stability make the drug to treat the glucose-related diseases in absence of insulin. By the observation in future prospects, the chitosan-loaded nanoparticles have the potency on cancer therapy.

Keywords: *Terminalia chebula,* chitosan nanoparticles, glucose tolerance, *in vitro* technique, antidiabetic activity.

AIMS AND BACKGROUND

Deacetylating chitin produces chitosan, a semi-synthetic substance made of acetylated and deacetylated monomers of glucosamine and N-acetyl-glucosamine that are joined by β-(1,4)-glycosidic linkages. The chitin extraction was obtained from the crustacean exoskeleton components such as crabs and shrimps. The chitosan is

* For correspondence.

consisting of β-(1,4)-linked D-glucosamine residues with the randomly acetylated amino group[1]. They are composed of natural polymer with the combination of synthetic and protein polymer. The chitin functions as a structural polysaccharide and is the healthy benefits of functional ingredients. The encapsulation of the drugs is being a major role in protecting the molecules efficiency. The Tripolyphosphate (TPP) is used in the preparation of the chitosan. They are the charged nanomolecular particles that are based on the interaction between the ionotropic gelation and the groups of negatively charged TPP. The solid colloidal particles are in the range from 10–1000 nm[2]. In the antidiabetic activity *T. chebula* plays an undifferentiated role with the seed efficiency with the reduction in the blood glucose level in the diabetic patients for long term[3]. α-Amylase and α-glycosidase have been tested for their antidiabetic activity[4,5]. *In vitro* the drugs was treated with 3T3 cell line for the proliferation and resistance can be observed[6].

EXPERIMENTAL

Collection and preparation of Terminalia chebula extract. The *T. chebula* fruits were collected from market and then ground to to fine dust particles. 5 g of ground powder was mixed with 50 ml of water and kept in shaker for 48 h. The mixture was filtered and dark black-brown liquid extract was obtained. The filtrate was stored in the refrigerator for further use.

Preparation of cross-linking of the required media. 2.4 g of chitosan were taken in a conical flask. Then 200 ml of deionised water were added and mixed till it got dissolved. Then 4% of acetic acid aqueous solutions was added drop by drop with the syringe on running magnetic stirrer at 37°C for 4 h until a clear product was obtained. The 0.4% of TPP solution was added drop wise in the chitosan solution under magnetic stirring at 800 rpm and 37°C (Refs 7 and 8). After 4 – 8 h of stirring, while on running magnetic stirrer, the *T. chebula* aqueous fruits extract was added dropwise by syringe till the full extract got bind with the chitosan nanoparticles. Then, the compound mixture was again kept on magnetic stirrer for 18 h for the cross-linking[9].

CHARACTERISATION OF CHITOSAN NANOPARTICLES

Ultraviolet-vis. Spectroscopy (*UV-Vis*). The UV-Vis analysis was done in between the range of 300–700 nm using Ultraviolet-Visible Spectroscopy.

Fourier Transform Infrared (*FTIR*) *Spectra*. The chitosan nanoparticles sample performance analysis by FTIR was done by attenuated total reflectance Fourier transform infra-red spectrometer [(ATR-FTIR) from VIT, Chennai, India]. The sample extracts were recorded with the verified infrared spectral range within 500 to 4000 cm^{-1} and with 4 cm resolution in the 10-scan absorbance mode been set at room temperature.

Field-emission Scanning Electron Microscope (*FE-SEM*) *observation*. Chitosan nanoparticles surface morphology can be studied by using FE-SEM. For the analysis

purpose, preparation of thin film was done on the surface of glass slide and dried for overnight inside the laminar air flow chamber. The gold coating was done by using sputter coater for the analysis and the verification of the sample images with different accelerated voltage ranges from 25 -50 kV. The sample was examined with the model [(Model – Quattro S; Make- Thermo Fisher Scientific, USA) from VISTAS, Chennai, India], for Field Emission Scanning Electron Microscope (FESEM) with Energy Dispersive X-Ray Spectrometer (EDS). The FE-SEM; EDS were examined in the Quanta 400 and through a sputter the double-sided adhesive tape was observed at 50 mA for 5–10 min.

X-ray diffraction (*XRD*) *analysis*. X-ray diffraction (XRD) analysis was done to evaluate crystallinity of *T. chebula* and chitosan cross-linked compound. Data were collected at a scan rate of 4 degree per min with the scan angle from 10° to 60°. Powder X-ray diffraction (p-xrd) [(2θ range-5 to 130) (Model- Smart Lab SE X-Ray; Make- Rigaku, Japan) from VISTAS, Chennai, India]. The XRD data were calculated from crystalline index for chitin determination. The chitosan sample was poured on a Petri dish and was finally dried at 75°C for 16–18 hr under vacuum.

Dynamic Light Scattering (*DLS*) *analysis*. The dynamic light scattering (DLS) analysis was used to analyse nanoparticles. The 400 ml sample mixture was sonicated for 4 min and then the analysis was carried out. The nanoparticles average size was measured at the temperature of 20–30°C (Ref. 10).

Alpha-amylase inhibition assay. According to the Bernfield method, the determination of α-amylase inhibition was carried out in modified version[11]. In test tubes the sample extracts in the range of 20, 40, 60, 80, and 100 µl/ml were ordered accordingly. One test tube was taken as control. The reaction mixture was composed of the solution, 8 µl of α-amylase were dissolved in 40 µl of phosphate buffer saline solution (PBS, 80mM, pH – 6.9) and incubated at 37°C for 20 min (Ref. 12). Then the reaction was incubated by adding 150 µl Dinitrosalicylic acid (DNS) reagent to the reaction mixture boiling at 100°C for 10 min (Ref. 13). After cooling at room temperature, absorbance reading was taken at 540 nm recorded by UV-Vis. spectroscopy. The experiments were performed in triplicates[14].

The inhibition percentage was calculated by the following equation:

$$\text{inhibition (\%)} = [(\text{Abs1} - \text{Abs2})/\text{Abs1}] \times 100,$$

where Abs1 is the absorbance of the sample and Abs2 – the absorbance of the control.

Alpha-glycosidase inhibition assay. In 96 well plates, five different concentrations of fraction with one control and the sample extracts in the range from 20, 40, 60, 80, and 100 µl/ml were ordered accordingly[15]. The reaction mixtures composed of the solution, 8 µl of α-glycosidase were dissolved in 40 µl of phosphate buffer saline solution (PBS, 80 mM, pH – 6.9) and incubated at 37°C for 10 min. Then the reaction was incubated by adding 15 µl P-NPG (2.5 mM) reagent added as a substrate and incubated at a

temperature of 37°C for 30 min. The stopping of the reaction was done by applying or adding 40 µl of Na_2CO_3 (80 mM) reagent. The released *p*-nitrophenol absorbance was measured at 405 nm using Multiplate reader tool[16]. The experiments were performed in triplicates[17]. The inhibition percentage was calculated by the following equation:

$$\text{inhibition (\%)} = [(\text{Abs1} - \text{Abs2})/\text{Abs1}] \times 100,$$

where Abs1 is the absorbance of the sample and Abs2 – the absorbance of the control.

Cell culture maintenance. Musmusculus cell from mouse embryo fibroblast cell line were obtained from the National Centre for Cell Sciences (NCCS), Pune, India. This is a suitable transfection host cell line. The highly sensitive 3T3 cell line is been opt for sarcoma virus focus formation. The Dulbecco's Modified Eagle Medium (DMEM) was added in the cell line for the proper growth. The other growth medium Fetal Bovine Serum (FBS) was added at a concentration of 10–15%; 150 µl of antibiotic and 100 µl of trypsin. The appropriate 37°C was maintained with the suspension to new culture vessel and 5% CO_2 incubator[18].

Glucose metabolism assay. According to the method described by Janjic and Wollheim, the glucose metabolism assay in 3T3 cells using MTT or tetrazolium colorimetric assay was carried out. For the culturing of the cells, the Dulbecco's Modified Eagle Medium containing 10% of FBS was used. The 96 well plates were seeded with a density of 6000 to 8000 cells per well with a volume of 150 µl. Treated chitosan with cell line were left overnight and allow to attain 70% confluence. Then the cells were suspended with 1.5% glucose and incubated for 48 h to get attached, the fruits extract with different concentrations of 20, 40, 60, 80, and 100 µl/ml and the PBS which serve as a control in the presence of glucose (30 mM)[19]. After 48 h of incubation at room temperature of 37°C, the medium was removed from the cells. Then 150 µl DMEM medium containing 10% of FBS and 1.0 mg/ml MTT were added. The additional incubation was carried out for 5 h at 37°C. The purple formazan of MTT crystal was dissolved in 250 µl/well. The absorbance value of the plate was measured at 540 nm using Multiplate Reader[20,21]:

$$\text{percent increase} = t/c \times 100,$$

where t is the absorbance of tested cell substance and c – the absorbance of the control cells.

In vitro ANTIDIABETIC ACTIVITY STUDY

The cell viability studies were performed in triplicates. The fibroblastic cells were grown in Dulbecco's Modified Eagle Medium. The 96 well plate was seeded with a density of 6000 to 8000 cells per well and incubated for 24 h at 37°C with addition of 5% CO_2. The glucose metabolism MTT assay was induced in the diabetic cells and incubated in CO_2 incubator for 48 h. The absorbance value of the plate was measured at 540 nm using Multiplate Reader. The sample was analysed in triplicate manner.

The antidiabetic activity was directly or indirectly proportional to the number of viable cells[18,22]:

$$\text{cell viability (\%)} = \frac{\text{absorbance of treated cells}}{\text{absorbance of control cells}} \times 100.$$

RESULTS AND DISCUSSION

CHARACTERISATION OF CHITOSAN NANOPARTICLES

Ultraviolet-Visible spectroscopy (*UV-Vis*). The absorption peak in Fig. 1 shows the chitosan nanoparticle formation at 407 nm in the range between 300 and 700 nm.

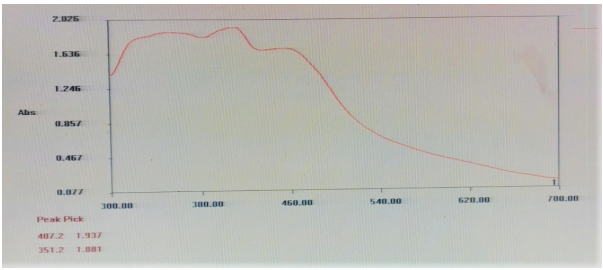

Fig. 1. UV absorption spectrum of chitosan nanoparticles

Fourier Transform Infrared (*FTIR*) *Spectra.* The FT-IR analysis (Figs 2 and 3) determines the *Terminalia chebula* loaded chitosan nanoparticles. In Fig. 2, in the spectrum of chitosan, the peak obtained at 339.28 cm^{-1} determines the presence of Cl in the bending vibrating form. The number of bands that has created vibrating effects in the region between 1636.19–1279.62 cm^{-1} determines the presence of carboxylic acid in the bending and in the hinge region of Fig. 2. The curve in Fig. 3 determines the presence of oxygen that has a vibrating effect on the region within the range of 3342.54 cm^{-1} denoting N–H and –OH functional groups and another area which affects the graph with presence of carbon in the compound[7].

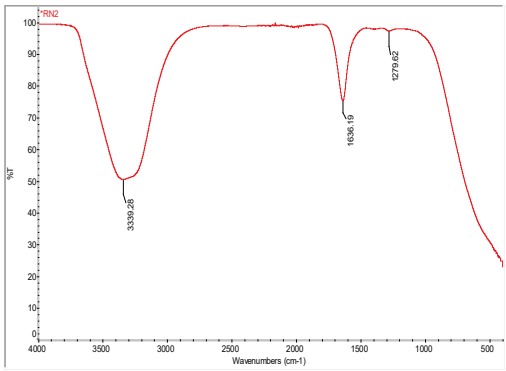

Fig. 2. FT-IR graph for chitosan nanoparticles

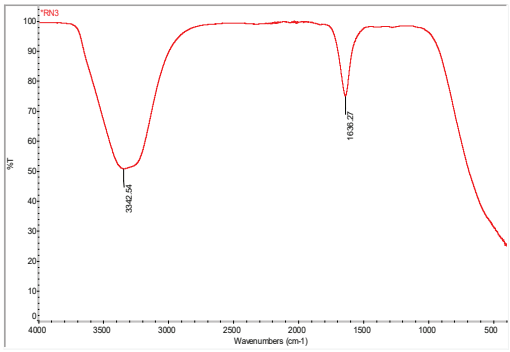

Fig. 3. FT-IR graph for cross-linked mixture (chitosan nanoparticles and fruit extract)

Field-emission Scanning Electron Microscope (*FE-SEM*) *Analysis.* The FE-SEM result in Fig. 4 shows the spherical morphology with clear and smooth surface of the nanoparticles[23]. The magnificence of the chitosan nanoparticles with the mixture of *Terminalia chebula* measured in 'image a' was 10 µm, and 'image b' – 20 µm. The crystalline forms determine the chitosan nanoparticles efficiency. The verification of the molecules was identified at suitable conditions[24,25].

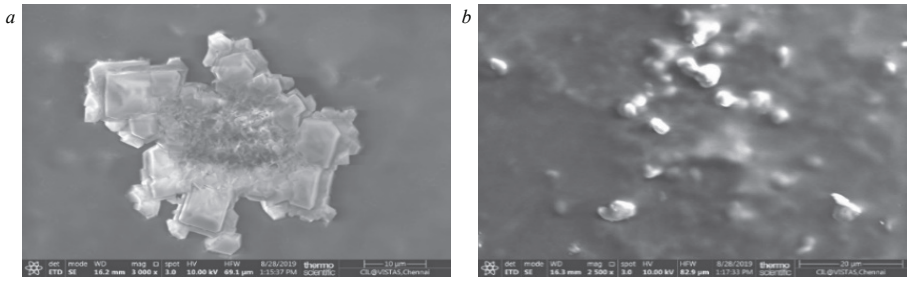

Fig. 4. Images (*a*) and (*b*) Field-emission Scanning Electron Microscope (FE-SEM) view of chitosan nanoparticles

Energy Dispersive X-Ray Spectroscopy (*EDS*). The Energy Dispersive X-Ray Spectrometer (EDS) in Fig. 5 describes the results of the presence of carbon, chloride, oxygen, silicon, nitrogen, calcium, potassium, chlorine and aluminum. The carbon and chloride atom molecular weights were in the range of 4 K which indicates the higher spectrum[26]. The molecular weight of oxygen is between the middle of the 3 to 4 K which indicates the moderate spectrum range. The range for silicon is between 1–2 K (Refs 27 and 28).

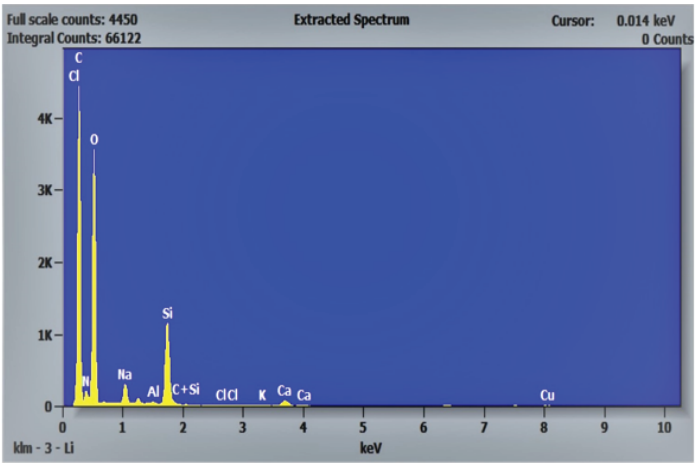

Fig. 5. Energy Dispersive X-Ray spectrum of chitosan nanoparticles

X-ray Diffraction (XRD) analysis. The XRD analysis in Fig. 6 shows the amorphous structure which is the characteristic feature that describes the presence of chitosan nanoparticles[29,30].

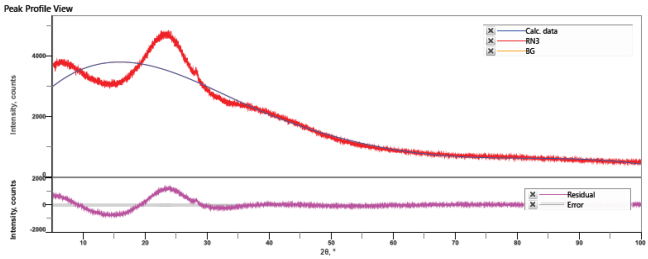

Fig. 6. XRD graphs of chitosan nanoparticles and drug extract

Dynamic Light Scattering (*DLS*) *analysis*. The value measured for the zeta potential for the chitosan nanoparticles was found to be around 62.3 mV (Fig. 7), which indicates the good stability of nanoparticles. The concentration obtained from particle size was at 224 nm for the verification of chitosan nanoparticles that been cross linked with drug sample[31,32].

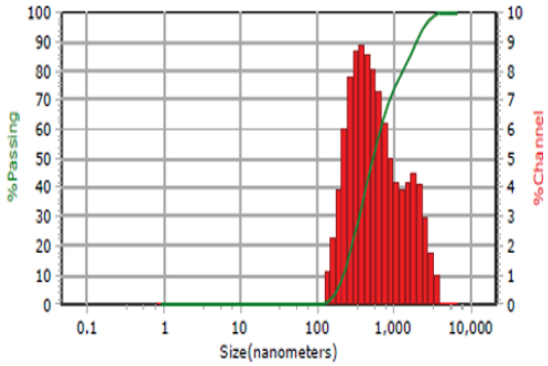

Fig. 7. Particle size distribution and zeta potential graph

Alpha-amylase inhibition assay. The graph from Fig. 8 visualises verification of compounds that vary in three different concentration levels. The most efficient is the combined complex of nanoparticle with fruit extract with inhibition potential of 84.56 + 1.05%. The readings have been taken through UV-Vis Spectrophotometer at an absorbance of 540 nm (Refs 30, 33, 34).

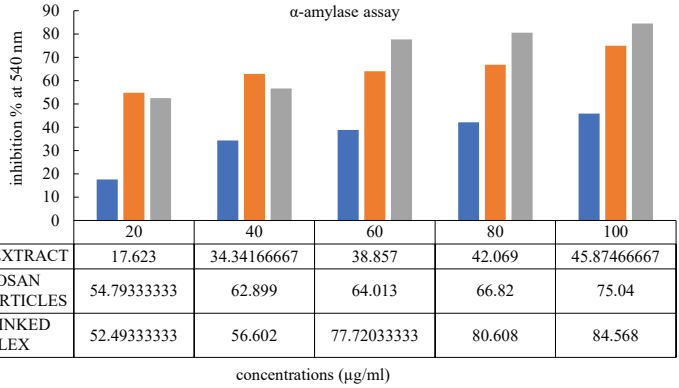

	20	40	60	80	100
FRUITS EXTRACT	17.623	34.34166667	38.857	42.069	45.87466667
CHITOSAN NANOPARTICLES	54.79333333	62.899	64.013	66.82	75.04
CROSS-LINKED COMPLEX	52.49333333	56.602	77.72033333	80.608	84.568

Fig. 8. Graphical representation of alpha-amylase inhibition assay

Alpha-glycosidase inhibition assay. The graph from Fig. 9 visualises the verification of compounds in three different concentration levels. Fruit extract has got a maximum inhibition of 95.691%, chitosan nanoparticles have an inhibition potential of 39.772%, combined nanoparticle and fruit extract has inhibited 90.542% α-glucosidase at 100 µg/ml, respectively. The readings have been taken through Multiplate reader at an absorbance of 405 nm[30,34].

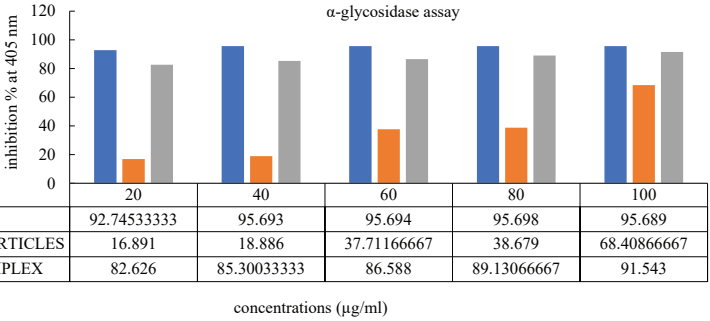

	20	40	60	80	100
FRUITS EXTRACT	92.74533333	95.693	95.694	95.698	95.689
CHITOSAN NANOPARTICLES	16.891	18.886	37.71166667	38.679	68.40866667
CROSS-LINKED COMPLEX	82.626	85.30033333	86.588	89.13066667	91.543

Fig. 9. Graphical representation of alpha-glycosidase inhibition assay

In vitro GLUCOSE METABOLISM BY MTT ASSAY ANALYSIS AND CELL VIABILITY STUDY

Glucose metabolism by MTT assay analysis. In Fig. 10, the control condition shows the better morphology of the cell line which seems to be very adequate for the treatment of blood glucose-related diseases and the binding of the cells with the drugs are clearly observed. At the 20 µg/ml concentration the cells start binding with the drug which indicates the efficiency of the drug to treat with the cell line (3T3 fibroblastic)[35].

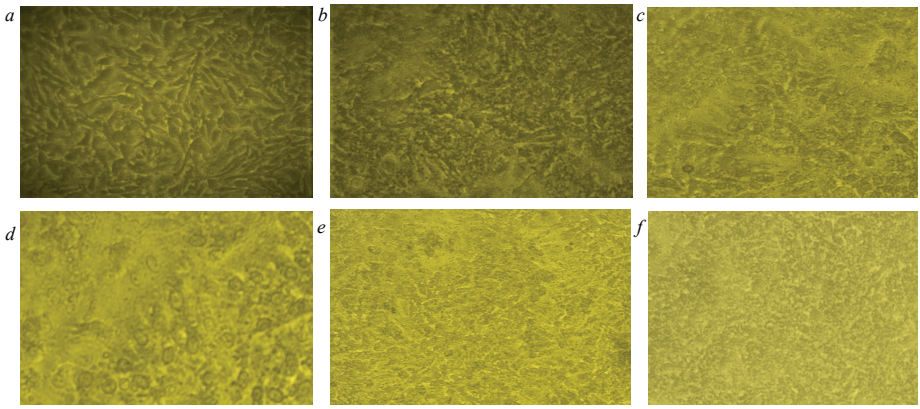

Fig. 10. Cell line morphology and the binding with the ant diabetic drugs and determination of the cells viability of the cells: *a* – the control condition; *b* – the concentration of cells in 80 µl; *c* – the concentration of cells in 60 µl; *d* – the concentration of cells in 40 µl; *e* – the concentration of cells in 20 µl; *f* – the concentration of cells in 100 µl

Cell viability study. In Fig. 11, the cell viability range determines the cell death condition. At 100 µg/ml 48% of the cell population were viable, 52% of the cells died. When concentration decreases cell viability decreases.

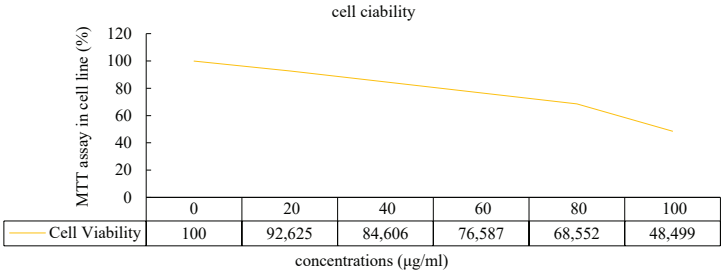

Fig. 11. Cell viability study by MTT assay

CONCLUSIONS

In the present work is demonstrated that the chitosan nanoparticles have the potential effects on type 2 diabetic activity. The XRD patterns observed for chitosan nanoparticles have been verified under optimised conditions but the ranges determine the nanoparticle trace. The characterisation of chitosan nanoparticles was performed by UV-Vis spectroscopy at 407 nm, SEM, EDS, EM analysis showed the morphology of nanoparticle which was observed as homologous and spherical in shape. The DLS analysis of zeta potential for chitosan nanoparticles was 62.3 mV. The particle size is 220 nm in DLS analysis. In the FT-IR analysis, the presence of carboxylic acid and N-OH functional groups for both the chitosan and the cross-linking drug was proved. The glucose metabolism and the viability of cells have been performed through MTT assay. Here the 3T3 fibroblastic cell line has been used for *in vitro*. The glucose metabolism also confined that the drug morphology and the binding stability make the drug to treat the glucose related diseases in the absence of insulin.

ACKNOWLEDGEMENTS

The authors are thankful to the Vels Institute of Science, Technology and Advanced Studies (VISTAS) for providing a facility to carry out this work.

REFERENCES

1. M. AGARWAL, M. K. AGARWAL, N. SHRIVASTAV et al.: Preparation of Chitosan Nanoparticles and Their *in-vitro* Characterization. Int J Life Sci Res, **4** (2), 1713 (2018).
2. J. KREUTER: Nanoparticulate Systems for Brain Delivery of Drugs. J Adv Drug Del Rev, **47** (1), 65 (2001).
3. S. COHEN, E. FLESCHER: Methyl Jasmonate: a Plant Stress Hormone as an Anticancer Drug. Phytochemistry, **70** (13–14), 1600 (2009).
4. F. E. KOEHN, G. T. CARTER: The evolving Role of Natural Products in Drug Discovery. Nat Rev Drug Discov, **4** (3), 206 (2005).
5. A. BAG, S. K. BHATTACHARYYA, R. R. CHATTOPADHYAY: The Development of *Terminalia chebula* Retz. (Combretaceae) in Clinical Research. Asian Pac J Trop Biomed, **3** (3), 244 (2003).

6. S. H. SUKHDEV, M. DEEPAK, G. V. R. JOSEPH, S. JOSEPH, G. NAGAR: Indian Herbal Pharmacopoeia. Vol II. Jammu Tawi: IDM, Mumbai and RRL, CSIR, 1999, p. 154.
7. F. N. HAFDANI, N. SADEGHINIA, A Review on Application of Chitosan as a Natural Antimicrobial. Int J Pharm Pharm Sci, **5** (2), 46 (2011).
8. C. PREGO, P. PAOLICELLI, B. DIAZB et al.: Chitosan-based Nanoparticles for Improving Immunization against Hepatitis B Infection. Vaccine, **28** (14), 2607 (2010).
9. A. R. PATEL, P. VAVIA: Evaluation of Synthesized Cross-linked Polyvinyl Alcohol as Potential Disintegrant. J Pharm Pharm Sci, **13** (2), 114 (2010).
10. S. A. AGNIHOTRI, N. N. MALLIKARJUNA, T. M. AMINABHAVI: Recent Advances on Chitosan-based Micro- and Nanoparticles in Drug Delivery. J Control Release, **100** (1), 5 (2004).
11. S. GHOSH, M. AHIRE, S. PATIL et al.: Antidiabetic Activity of Gnidiaglauca and Dioscoreabulbifera: Potent Amylase and Glucosidase Inhibitors. Evidence-based Complementary and Alternative Medicine (eCAM), **1**, (2012).
12. S. PRAKASH, S. DESHWAL: Alpha and Beta Amylase Activity of *Fagopyrum esculentum* (Buckwheat): a Medicinal Plant. Janaki Medical College Journal of Medical Science, **1** (1), 53 (2013).
13. K. SUTHINDHIRAN, M. A. JAYASRI, K. KANNABIRAN: α-Glucosidase and α-amylase Inhibitory Activity of Micromonospora sp. VITSDK3 (EU551238). Int J Integr Biol, **6** (3), 115 (2009).
14. M. BHAT, S. S. ZINJARDE, S. Y. BHARGAVA et al.: Antidiabetic Indian Plants: a Good Source of Potent Amylase Inhibitors. Evidence-Based Complementary and Alternative Medicine (eCAM), **1**, (2011).
15. E. GALIP, H. AFIK, O. OMER et al.: Leukotrienes in Cerulein-induced Acute Pancreatitis in Rats and Effect of Octreotide. Turk J Gastroenterol, **10** (1), 40 (1999).
16. S. P. SANAP, S. GHOSH, A. M. JABGUNDE et al.: Synthesis, Computational Study and Glycosidase Inhibitory Activity of Poly Hydroxylated Conidine Alkaloids – a Bicyclic Imino Sugar. Org Biomol Chem, **8** (14), 3307 (2010).
17. P. BALASHANMUGAM, P. DURAI, M. D. BALAKUMARAN et al.: Phyto Synthesized Gold Nanoparticles from *C. roxburghii* DC. Leaf and Their Toxic Effects on Normal and Cancer Cell Lines. J Photochem Photobiol B: Biology. **1**, 163 (2016).
18. P. A. HALBAN, G. A. PRAZ GA, C. B. WOLLHEIM: Abnormal Glucose Metabolism Accompanies Failure of Glucose to Stimulate Insulin Release from a Rat Pancreatic Cell Line (RIN m5F). Biochem J, **212**, 439 (1983).
19. D. JANJIC, C. B. WOLLHEIM: Islet Cell Metabolism Is Reflected by the MTT (Tetrazolium) Colorimetric Assay. Diabetologia, **35** (5), 482 (1992).
20. W. MALAISSE: Defects of Signal Transduction in a Tumoral Islet Cell Line. In: Molecular Biology of the Islets of Langerhans (Ed. H. Okamoto). University Press, Cambridge, 1990. 315 p.
21. T. MOSSMANN: Rapid Colorimetric Assay for Cellular Growth and Survival: Application to Proliferation and Cytotoxicity Assays. J Immunol Methods, **65**, 55 (1983).
22. N. HASHEMINEJAD, F. KHODAIYAN, M. SAFARI: Improving the Antifungal Activity of Clove Essential Oil Encapsulated by Chitosan Nanoparticles. Food Chem, **275**, 113 (2019).
23. D. RAGHUNANDAN, S. BASAVARAJA, B. MAHESH et al.: Biosynthesis of Stable Poly Shaped Gold Nanoparticles from Microwave-exposed Aqueous Extracellular Anti-malignant Guava (*Psidium guajava*) Leaf Extract. Nano biotechnology, **5**, 34 (2009).
24. P. MANIMEKALAI, R. DHANALAKSHMI, R. MANAVALAN: Preparation and Characterization of Ceftriaxone Sodium Encapsulated Chitosan Nanoparticles. Int J Appl Pharm, **9**, 10 (2017).
25. K. ARUNACHALAM, S. ANNAMALAI, H. SHANMUGASUNDARAM: One-step Green Synthesis and Characterization of Leaf Extract-mediated Biocompatible Silver and Gold Nanoparticles from Memecylonumbellatum. Int J Nanomed, **8**, 1307 (2013).
26. M. E. ABDULRAHMAN, N. C. CHRISTOPHER, M. MERVIN, A. A. HUSSEIN: Large Scale Screening of Southern African Plant Extracts for the Green Synthesis of Gold Nanoparticles Using Microtitre-Plate Method. Molecules, **8**, 8 (2016).

27. E. L. RODRIGUEZ, R. P. INIGUEZ, R. NAVARRO, R. HERRERA-URBINA et al.: Synthesis of Silver Nanoparticles Using Reducing Agents Obtained from Natural Sources (*Rumex hymenos*epalus Extracts). Nanoscale Res Lett, **8**, 318 (2013).
28. D. N. MOHAMMADPOUR, R. ESKANDARI, M. R. AVADI, H. ZOLFAGHARIAN et al.: Preparation and *in vitro* Characterization of Chitosan Nanoparticles Containing *Mesobuthu eseupeus* scorpion venom as an antigen delivery system. J Venomous Animals and Toxins including Tropical Diseases (JVAYiTD), **18** (1), 44 (2012).
29. H. WU, Z. JUXIN: Chitosan-based Zinc Oxide Nanoparticle for Enhanced Anticancer Effect in Cervical Cancer: a Physicochemical and Biological Perspective. Saudi Pharm J, **2**, 205 (2018).
30. M. O. M TANIRA: Antidiabetic Medicinal Plants: a Review of the Present Status and Future Directions. Int J Diabetes, **29** (1), 15 (1994).
31. D. BHARATHI, R. RANJITHKUMAR, B. CHANDARSHEKAR, V. BHUVANESHWARI: Preparation of Chitosan Coated Zinc Oxide Nanocomposite for Enhanced Antibacterial and Photocatalytic Activity: as a Bionanocomposite. Int J Biol Macromol, **15**, 989 (2019).
32. R. L. RHABASO, J. L CHIASSON: α-Glucosidase Inhibitors. In: International Textbook of Diabetes Mellitus (Eds R. A. Defronzo, E. Ferrannani, H. Keen, P. Zimmet). 3rd ed. John Wiley and Sons Ltd., UK, 1, 2004. 901 p.
33. D. V. MANAM, S. MURUGESAN: Biological Synthesis of Silver Nanoparticles from Marine Alga *Colpomenia sinuosa* and Its in vitro Anti-diabetic Activity. American Journal of Bio-pharmacology Biochemistry and Life Sciences (AJBBL), **3** (1), 1 (2014).
34. A. STRASSER, L. O'CONNOR, V. M. DIXIT: Apoptosis Signaling. Ann Rev Biochem, **69**, 217 (2007).
35. M. ELAD, J. ANNA, K. TATIANA et al: Methyl Jasmonate Reduces the Survival of Cervical Cancer Cells and Down Regulates HPV E6 and E7, and Surviving. Cancer Lett, 319 (2012).

Received 8 November 2022
Revised 15 December 2022